Synaptotagmin-1–, Munc18-1–, and Munc13-1–dependent liposome fusion with a few neuronal SNAREs

Karolina P. Stepien[a,b,c] and Josep Rizo[a,b,c,1]

[a]Department of Biophysics, University of Texas Southwestern Medical Center, Dallas, TX 75390; [b]Department of Biochemistry, University of Texas Southwestern Medical Center, Dallas, TX 75390; and [c]Department of Pharmacology, University of Texas Southwestern Medical Center, Dallas, TX 75390

Edited by William Wickner, Dartmouth College, Hanover, NH, and approved December 9, 2020 (received for review September 13, 2020)

Neurotransmitter release is governed by eight central proteins among other factors: the neuronal SNAREs syntaxin-1, synaptobrevin, and SNAP-25, which form a tight SNARE complex that brings the synaptic vesicle and plasma membranes together; NSF and SNAPs, which disassemble SNARE complexes; Munc18-1 and Munc13-1, which organize SNARE complex assembly; and the Ca^{2+} sensor synaptotagmin-1. Reconstitution experiments revealed that Munc18-1, Munc13-1, NSF, and α-SNAP can mediate Ca^{2+}-dependent liposome fusion between synaptobrevin liposomes and syntaxin-1–SNAP-25 liposomes, but high fusion efficiency due to uncontrolled SNARE complex assembly did not allow investigation of the role of synaptotagmin-1 on fusion. Here, we show that decreasing the synaptobrevin-to-lipid ratio in the corresponding liposomes to very low levels leads to inefficient fusion and that synaptotagmin-1 strongly stimulates fusion under these conditions. Such stimulation depends on Ca^{2+} binding to the two C_2 domains of synaptotagmin-1. We also show that anchoring SNAP-25 on the syntaxin-1 liposomes dramatically enhances fusion. Moreover, we uncover a synergy between synaptotagmin-1 and membrane anchoring of SNAP-25, which allows efficient Ca^{2+}-dependent fusion between liposomes bearing very low synaptobrevin densities and liposomes containing very low syntaxin-1 densities. Thus, liposome fusion in our assays is achieved with a few SNARE complexes in a manner that requires Munc18-1 and Munc13-1 and that depends on Ca^{2+} binding to synaptotagmin-1, all of which are fundamental features of neurotransmitter release in neurons.

neurotransmitter release | synaptic vesicle fusion | synaptotagmin-1 | membrane fusion | reconstitution

Brain function depends on the ability of neurons to communicate through neurotransmitters that are released by Ca^{2+}-evoked synaptic vesicle exocytosis. This process involves tethering of synaptic vesicles to the plasma membrane at presynaptic active zones, a priming reaction(s) that leaves the vesicles ready for release and fast (<1 ms) fusion of the vesicle and plasma membranes upon Ca^{2+} influx into a presynaptic terminal (1). Extensive studies have shown that release is controlled by a sophisticated protein machinery that includes the synaptic vesicle SNAP receptor (SNARE) synaptobrevin and the plasma membrane SNAREs syntaxin-1 and SNAP-25 as central components (2, 3). These proteins drive exocytosis by assembling into highly stable SNARE complexes that form a four-helix bundle and bring the two membranes together (4–7). The SNAREs are recycled by *N*-ethylmaleimide sensitive factor (NSF) and soluble NSF attachment proteins (SNAPs), which disassemble the cis-SNARE complexes resulting after fusion (4, 8) and any four-helix bundle formed by the SNAREs before fusion (9–11). SNARE complex assembly is orchestrated in an NSF-SNAP–resistant manner by Munc18-1 and Munc13-1 (9, 10) through a mechanism whereby Munc18-1 binds to a self-inhibited "closed" conformation of syntaxin-1 (12, 13) and to synaptobrevin, forming a template for SNARE complex formation (14–17), while Munc13-1 bridges the two membranes (18) and opens syntaxin-1 (19, 20). This mechanism ensures that exocytosis occurs through a highly regulated pathway where Munc13-1 and associated proteins act as master regulators of presynaptic plasticity (21, 22). Fast, Ca^{2+}-dependent neurotransmitter release is triggered by the synaptic vesicle protein synaptotagmin-1 (Syt1), which acts as a Ca^{2+} sensor through interactions of its two C_2 domains (referred to as C_2A and C_2B) with Ca^{2+} and phospholipids (23, 24) in a tight interplay with the SNAREs (25, 26). However, despite the advances made in defining the functions of these proteins, it is still unknown how their actions are integrated to induce fast, Ca^{2+}-dependent membrane fusion.

Approaches aimed at recapitulating synaptic vesicle fusion with reconstituted proteoliposomes provide a powerful tool to decipher mechanistic features of this complex system, but it is important to realize that liposome fusion can occur through nonphysiological pathways. Hence, establishing correlations between the results of fusion assays and physiological data are crucial to verify that the assays reproduce to some extent basic features of synaptic vesicle fusion (2). Pioneering reconstitution studies suggested that the neuronal SNAREs alone or together with Syt1 constitute a minimal membrane fusion machinery (27, 28), but these studies did not include Munc18-1 or Munc13s, which are essential for neurotransmitter release in vivo (29–31). This apparent paradox was resolved by reconstitution assays

Significance

Neurotransmitter release is crucial for neuronal communication. Reproducing the steps that lead to neuronal exocytosis with lipid vesicles and purified proteins provides a powerful strategy to elucidate the molecular mechanisms underlying release. Previous studies showed that reconstitution experiments including Munc18-1, Munc13-1, NSF, α-SNAP, and the SNARE proteins synaptobrevin, syntaxin-1, and SNAP-25, all of which are critical for neurotransmitter release, led to highly efficient vesicle fusion. However, synaptotagmin-1, the Ca^{2+} sensor that triggers release, did not have detectable effects in these fusion assays. We now show that, when the amounts of synaptobrevin and syntaxin-1 are lowered in otherwise analogous reconstitution experiments, vesicle fusion is strongly dependent on synaptotagmin-1, exhibiting several features that parallel those of neurotransmitter release in neurons.

Author contributions: K.P.S. and J.R. designed research; K.P.S. performed research; K.P.S. and J.R. analyzed data; and K.P.S. and J.R. wrote the paper.

The authors declare no competing interest.

This article is a PNAS Direct Submission.

[1]To whom correspondence may be addressed. Email: Jose.Rizo-Rey@UTSouthwestern.edu.

This article contains supporting information online at https://www.pnas.org/lookup/suppl/doi:10.1073/pnas.2019314118/-/DCSupplemental.

Published January 18, 2021.

showing that the SNAREs and Syt1 cannot induce liposome fusion in the presence of the SNARE complex disassembly machinery formed by NSF and α-SNAP and that, under these conditions, Munc18-1 and Munc13-1 are both required for liposome fusion because they mediate NSF-α-SNAP–resistant SNARE complex assembly (9, 10, 32). The physiological relevance of these liposome fusion assays has been supported by many correlations that have been established between the effects of mutations on fusion in vitro and on neurotransmitter release in neurons (16, 18, 22, 32, 33). However, a caveat of these assays is that highly efficient Ca^{2+}-dependent liposome fusion is observed in the presence of SNAREs, Munc18-1, Munc13-1, NSF, and α-SNAP even without Syt1; the Ca^{2+} dependence of fusion arises from Ca^{2+} binding to the Munc13-1 C_2B domain (32). These features are not necessarily in contradiction with the physiological properties of neurotransmitter release, as the time scale of these fusion assays (seconds) is much slower, and the Munc13-1 C_2B domain is involved in Ca^{2+}-dependent presynaptic plasticity (34). Moreover, Syt1 is essential for fast, synchronous release but not for slower forms of release (e.g., spontaneous or sucrose-induced) (35), in contrast to the absolute requirement of Munc18-1 and Munc13-1 for all forms of release (29, 31). Thus, Syt1 acts as an accelerator of synaptic vesicle fusion, but its stimulatory effect may not have been observable in the time scale of the fusion assays that included SNAREs, Munc18-1, Munc13-1, NSF, and α-SNAP (32). Nevertheless, the lack of overt effects of Syt1 in these assays hinders the analysis of the functional interplay between Syt1 and these proteins.

Reconstitution studies of yeast vacuolar fusion showed that the essential nature of the Rab protein Ypt7 could be recapitulated with proteoliposomes bearing physiological SNARE-to-lipid ratios but not at higher SNARE densities (36). In this context, the synaptobrevin-to-lipid and syntaxin-1–to–lipid ratios typically used in our liposome fusion assays, including Munc18-1, Munc13-1, NSF, and α-SNAP (1:500 and 1:800, respectively (32)), are considerably lower than those present in synaptic vesicles and the plasma membrane (37, 38). However, the neurotransmitter release machinery appears to tightly restrict the number of trans-SNARE complexes that are assembled between a vesicle and the plasma membrane, as neurotransmitter release can be triggered with as few as three SNARE complexes (39) and formation of a large number of such complexes might lead to uncontrolled fusion. Fluorescence resonance energy transfer (FRET) assays and structural data suggested that Munc13-1 restricts trans-SNARE complex assembly between synaptobrevin-liposomes and syntaxin-1–liposomes in the absence of Ca^{2+} but strongly stimulates assembly together with Munc18-1 in the presence of Ca^{2+} (10, 33). In vivo, such Ca^{2+}-dependent stimulation of SNARE complex assembly is expected to be much less efficient because the Ca^{2+} concentration is elevated during a very short

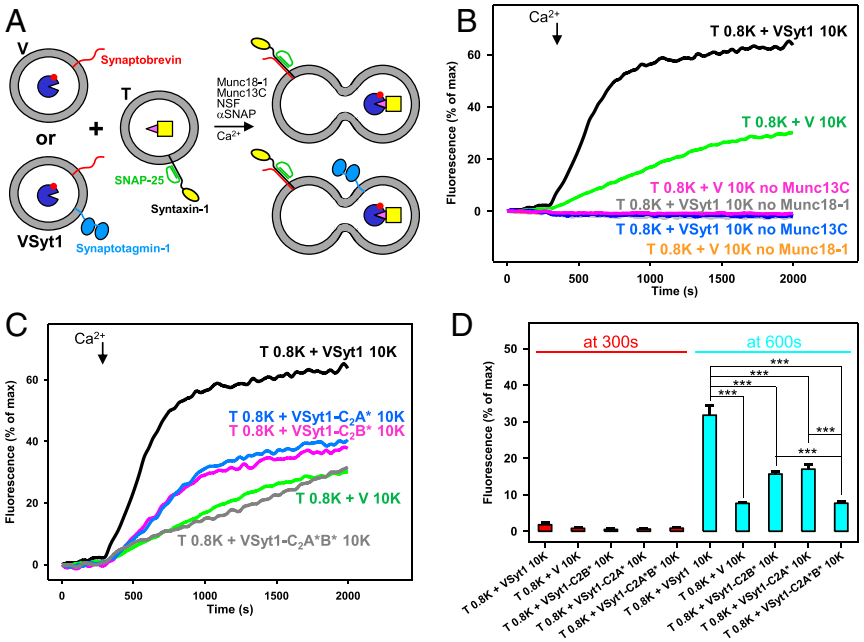

Fig. 1. Syt1 strongly stimulates liposome fusion at very low synaptobrevin-to-lipid ratios. (*A*) Diagram summarizing the content mixing assays used to test if Syt1 stimulates liposome fusion. V-liposomes containing synaptobrevin (red) or VSyt1-liposomes containing synaptobrevin and Syt1 (blue) are mixed with T-liposomes that contain syntaxin-1 (yellow) and SNAP-25 (green) and that have been preincubated with Munc18-1, NSF, and α-SNAP. Ca^{2+} is added after 300 s. The V- or VSyt1-liposomes contain trapped Cy5-strepatavidin (navy blue pie shape with red circle) and the T-liposomes contain trapped PhycoE-biotin (yellow square with pink triangle). Content mixing resulting from liposome fusion results in formation of a complex between Cy5-streptavidin and PhycoE-biotin, leading to an increase in Cy5 fluorescence emission intensity upon excitation of PhycoE due to FRET. Unlabeled streptavidin (not shown) is included outside the vesicles to ensure that the content mixing signal does not arise from leakiness. (*B*) Content mixing between V- or VSyt1-liposomes and T-liposomes was monitored from the increase in the fluorescence signal of Cy5-streptavidin trapped in the V- or VSyt1-liposomes caused by FRET with PhycoE-biotin trapped in the T-liposomes upon liposome fusion. The synaptobrevin-to-lipid ratio in V- and VSyt1-liposomes (V 10K and VSyt1 10K, respectively) was 1:10,000, the Syt1-to-lipid ratio in VSyt1-liposomes was 1:1,000, and the syntaxin-1–to–lipid ratio in the T-liposomes was 1:800 (T 0.8K). The assays were performed in the presence of 1 μM Munc18-1, 0.2 μM Munc13-1C, 0.4 μM NSF, 2 μM α-SNAP, 5 μM excess SNAP-25, and 5 μM streptavidin, except for the controls where Munc18-1 or Munc13-1C was omitted (no Munc18-1 or no Munc13-1C, respectively), as indicated by the color-coded labels. Experiments were started in the presence of 100 μM EGTA, and Ca^{2+} (600 μM) was added at 300 s. (*C*) Analogous content mixing assays monitoring fusion of T-liposomes with V-liposomes or VSyt1-liposomes containing WT Syt1 or Syt1 bearing mutations in the Ca^{2+}-binding sites of the C_2A domain (VSyt1-C_2A* 10K), the C_2B domain (VSyt1-C_2B* 10K), or both (VSyt1-C_2A*B* 10K). (*D*) Quantification of the content mixing assays shown in *C*. Bars represent averages of the normalized fluorescence intensities observed in the content mixing assays at 300 s (i.e., before Ca^{2+} addition) and at 600 s (i.e., 300 s after Ca^{2+} addition), performed in triplicates. Error bars represent SDs. Statistical significance and *P* values were determined by one-way ANOVA with the Holm–Sidak test (***$P < 0.001$).

time window after Ca^{2+} influx, and additional regulatory factors may limit the number of SNARE complexes that are preassembled. Thus, unhindered SNARE complex assembly promoted by Munc13-1, Munc18-1, and Ca^{2+} in the liposome fusion assays may mask a stimulatory role of Syt1. Such a role may become apparent by decreasing the SNARE-to-lipid ratio in the liposomes even further below physiological ratios. Moreover, having only a few SNAREs per liposome facilitates mechanistic studies of the steps that lead to release (10) and limits the number of trans-SNARE complexes that can be formed at each site of fusion between liposomes, which may help to better recapitulate the states of the release machinery that occur in vivo. However, it is unclear whether very low SNARE-to-lipid ratios are sufficient for liposome fusion in this minimal system.

The study presented here was designed to investigate whether liposome fusion can be achieved efficiently with a small number of neuronal SNAREs per liposome in a manner that depends not only on Munc18-1 and Munc13-1 but also on Syt1. For this purpose, we modified our previously developed reconstitution assays (9, 21, 32), exploring the effects of changing the SNARE-to-lipid ratios and of anchoring SNAP-25 on the syntaxin-1–liposomes, which is expected to facilitate SNARE complex assembly. We found that fusion of liposomes bearing a 1:10,000 synaptobrevin-to-lipid ratio with liposomes containing a 1:800 syntaxin-1–to–lipid ratio is inefficient in the presence of soluble SNAP-25, Munc18-1, Munc13-1, NSF, and α-SNAP, and that including Syt1 in the synaptobrevin-liposomes strongly stimulates fusion. Anchoring SNAP-25 on the syntaxin-1-liposomes dramatically enhanced fusion, yielding highly efficient fusion even in the absence of Ca^{2+} and Syt1. However, when we lowered the syntaxin–1-to–lipid ratio to 1:5,000, efficient fusion with liposomes bearing a 1:10,000 synaptobrevin-to-lipid ratio required Ca^{2+}, Syt1, and membrane anchoring of SNAP-25. Such fusion was disrupted by mutations in the Ca^{2+}-binding sites of the Syt1 C_2 domains, showing that fusion depends on Ca^{2+} binding to Syt1. These results reveal an intriguing synergy between Syt1 and SNAP-25 that is reminiscent of the synergy existing among Munc18-1, Munc13-1, NSF, and α-SNAP (21) and show that these proteins, together with Syt1 and a few SNARE complexes, can mediate efficient Ca^{2+}-dependent liposome fusion.

Results

Stimulation of Fusion by Syt1 at Low Synaptobrevin Densities. For the reconstitution experiments presented here, we used the methodology that was developed to monitor lipid and content mixing between proteoliposomes to study yeast vacuolar fusion (40) and that we adapted to investigate synaptic vesicle fusion (32) (Fig. 1*A*). The Munc13-1 fragment used in these studies rescues neurotransmitter release in Munc13-1/2 double knockout neurons (32) and spans the large C-terminal region that is conserved in all members of the Munc13 family, which includes the C_1, C_2B, MUN, and C_2C domains (referred to as Munc13-1C). In the experiments described below, we focused on monitoring content mixing between synaptobrevin-containing liposomes (V-liposomes) or synaptobrevin- and Syt1-containing liposomes (VSyt1-liposomes) and syntaxin-1-SNAP-25-containing liposomes (T-liposomes), which provides a more reliable means to demonstrate liposome fusion than lipid mixing (41). Under the standard conditions that we used in previous studies, with synaptobrevin-to-lipid ratio 1:500 and syntaxin-1–to–lipid ratio 1:800, the majority of fusion between V- and T-liposomes in the presence of Munc18-1, Munc13-1C, NSF, and α-SNAP occurred during the time elapsed between Ca^{2+} addition and acquisition of the first data point (32). Hence, it was not possible to observe stimulation of Ca^{2+}-dependent fusion by Syt1 in the second time scale of these bulk assays. To render the system less active and examine whether Syt1 can then stimulate fusion, we first lowered the synaptobrevin-to-lipid ratio to 1:10,000 in the V- and VSyt1-liposomes. Syt1 was reconstituted at a 1:1,000 protein-to-lipid (P:L) ratio, which is similar to that present in synaptic vesicles (37). We observed that fusion between V- and T-liposomes in the presence of Munc18-1, Munc13-1C, NSF, and α-SNAP (Fig. 1*B*, green curve) was much less efficient than that observed with a 1:500 synaptobrevin-lipid ratio (32), but, importantly, fusion was much more efficient when we used VSyt1-liposomes instead of V-liposomes (Fig. 1*B*, black curve). As expected, no fusion was observed in control experiments where we omitted Munc18-1 or Munc13-1C from the reactions (Fig. 1*B*).

The Syt1 C_2A and C_2B domains bind three and two Ca^{2+} ions, respectively, through a motif that includes five aspartate residues (42, 43), and neurotransmitter release is impaired when Ca^{2+} binding to either the C_2A or the C_2B domain is abolished by replacing three of these aspartate residues with alanines (44). To test whether fusion of VSyt1-liposomes with T-liposomes depends on Ca^{2+} binding to Syt1, we prepared VSyt1-liposomes bearing these mutations in C_2A, C_2B, or both (VSyt1-C_2A*, VSyt1-C_2B*, or VSyt1-C_2A*B*, respectively). The mutations in either the C_2A or C_2B Ca^{2+}-binding sites substantially impaired fusion (Fig. 1*C*, pink and blue curves; see Fig. 1*D* for quantification), and the impairments did not arise from unequal protein incorporation in the liposomes during reconstitution, as assessed by sodium dodecyl sulfate (SDS)-polyacrylamide gel electrophoresis (PAGE) (*SI Appendix*, Fig. S1). Moreover, mutation of the Ca^{2+}-binding sites of both C_2 domains abolished the stimulation of fusion by Syt1, as the low level of fusion observed with the VSyt1-C_2A*B* liposomes was comparable to that observed with the V-liposomes (Fig. 1*C*, gray and green curves, respectively; Fig. 1*D*). Overall, these results show that Syt1 strongly stimulates Ca^{2+}-dependent liposome fusion mediated by the neuronal SNAREs in the presence of Munc18-1, Munc13-1C, NSF, and α-SNAP and that such stimulation depends on Ca^{2+} binding to both C_2 domains of Syt1.

Membrane Anchoring of SNAP-25 Strongly Stimulates Liposome Fusion. In neurons, SNAP-25 is anchored on the plasma membrane through palmitoylation of four cysteines located in the linker region between its two SNARE motifs (45). In liposome fusion assays, however, SNAP-25 is commonly used as a soluble protein where the four cysteines are mutated to serines. We refer to this soluble protein as SNAP-25 for simplicity. Normally, T-liposomes are prepared with a fivefold excess of SNAP-25 over syntaxin-1, and the two proteins form heterodimers that are incorporated in the liposomes. Before the fusion assays, the T-liposomes are incubated with Munc18-1, NSF, and α-SNAP, which leads to disassembly of the syntaxin-1–SNAP-25 heterodimers and binding of Munc18-1 to closed syntaxin-1 (9). Since SNAP-25 is released from the liposomes during the preincubation and must rebind to form the SNARE complex, fusion is enhanced by addition of excess of SNAP-25 upon mixing the preincubated T-liposomes with the V-liposomes to increase SNAP-25 availability (9). Thus, we reasoned that anchoring SNAP-25 on the T-liposomes, mimicking its plasma membrane location in neurons, might provide an avenue to drastically increase the local concentration of SNAP-25 and enhance the efficiency of fusion in our assays. To test this notion, we followed a previously described approach involving dodecylation of the four cysteines of wild type (WT) SNAP-25 (referred to as dSNAP-25), which mimics palmitoylation and allows membrane anchoring, and substantially enhanced fusion caused by SNAREs alone (46).

First, we tested fusion between liposomes containing syntaxin-1 and dSNAP-25 (dT-liposomes), both at 1:800 P:L ratio, and V- or VSyt1-liposomes with a 1:1,000 P:L ratio for both synaptobrevin and Syt1 (Fig. 2*A*). For comparison, we also examined fusion of the standard T-liposomes bearing a 1:800 syntaxin-1–to–lipid ratio with the same V- and VSyt1-liposomes. Interestingly, while reactions with V- and T-liposomes in the presence of Munc18-1,

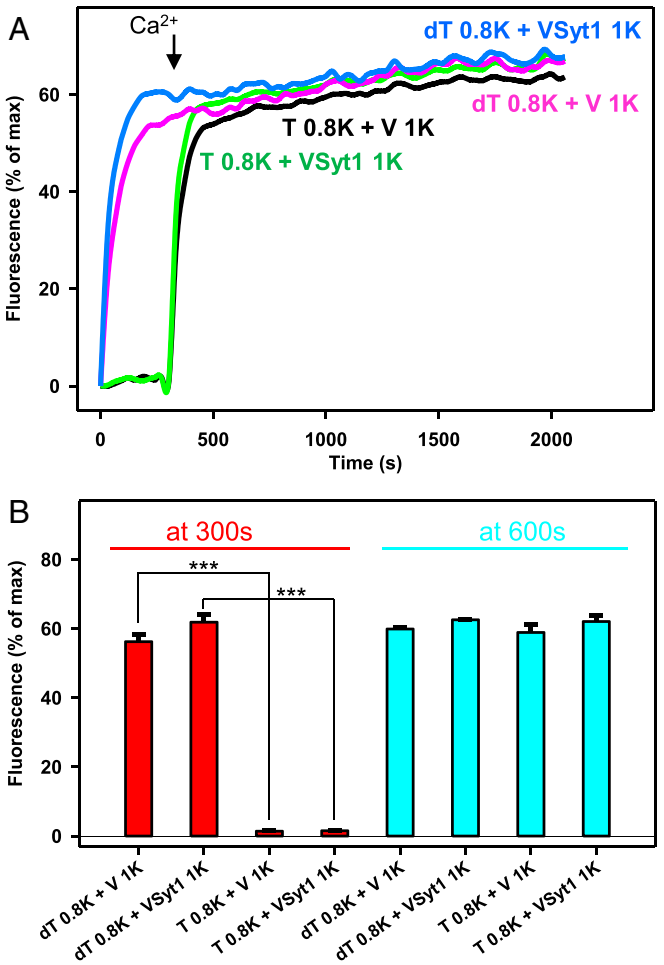

Fig. 2. Membrane anchoring of SNAP-25 dramatically enhances liposome fusion. (*A*) Content mixing between V- or VSyt1-liposomes (V 1K or VSyt1 1K, respectively) and T- or dT-liposomes (T 0.8K or dT 0.8K, respectively) was monitored from the increase in the fluorescence signal of Cy5-streptavidin trapped in the V- or VSyt1-liposomes caused by FRET with PhycoE-biotin trapped in the T- or dT-liposomes upon liposome fusion. The synaptobrevin-to-lipid ratio in V- and VSyt1-liposomes was 1:1,000, the Syt1-to-lipid ratio in VSyt1-liposomes was 1:1,000, the syntaxin-1–to–lipid ratio in the T- and dT-liposomes was 1:800, and the dSNAP-25–to–lipid ratio in the dT-liposomes was 1:800. The assays were performed in the presence of 1 μM Munc18-1, 0.2 μM Munc13-1C, 0.4 μM NSF, 2 μM α-SNAP, 5 μM excess SNAP-25 (only for experiments performed with T-liposomes), and 5 μM streptavidin. Experiments were started in the presence of 100 μM EGTA, and Ca^{2+} (600 μM) was added at 300 s. (*B*) Quantification of the content mixing assays shown in *A*. Bars represent averages of the normalized fluorescence intensities observed in the content mixing assays at 300 s (i.e., before Ca^{2+} addition) and at 600 s (i.e., 300 s after Ca^{2+} addition), performed in triplicates. Error bars represent SDs. Statistical significance and *P* values were determined by one-way ANOVA with the Holm–Sidak test (***$P < 0.001$).

Munc13-1C, NSF, and α-SNAP exhibited highly efficient fusion that was strictly Ca^{2+} dependent, we observed fast and efficient Ca^{2+}-independent fusion between V- and dT-liposomes (Fig. 2*A*, black and pink curves, respectively; see Fig. 2*B* for quantification). Similar results were obtained in assays performed with VSyt1-liposomes instead of V-liposomes (Fig. 2*A*, green and blue curves, respectively). Thus, enhancement of fusion by Syt1 could not be observed under these conditions of such high fusion efficiency.

We also tested how membrane anchoring of SNAP-25 affects fusion when the synaptobrevin-to-lipid ratio was decreased in the VSyt1-liposomes (keeping the Syt1-to-lipid ratio at 1:1,000) and/or the syntaxin-1–to–lipid ratio was decreased in the T-liposomes or dT-liposomes (keeping the dSNAP-25–to–lipid ratio at 1:800). Using a 1:5,000 synaptobrevin-to-lipid ratio and a 1:800 syntaxin-1–to–lipid ratio, we again observed highly efficient Ca^{2+}-independent fusion of VSyt1-liposomes with dT-liposomes, whereas fusion with T-liposomes was strictly Ca^{2+} dependent (Fig. 3*A*, green and black curves, respectively; quantification in Fig. 3*B*). When we decreased the syntaxin-1–to–lipid ratio to 1:2,500, we still observed Ca^{2+}-independent fusion of VSyt1-liposomes with dT-liposomes (Fig. 3*C*, pink curve), but it was less efficient than with a 1:800 syntaxin-1–to–lipid ratio, and fusion with T-liposomes was highly inefficient even upon addition of Ca^{2+} (Fig. 3*C*, blue curve; quantification in Fig. 3*D*). Finally, decreasing the syntaxin-1–to–lipid ratio to 1:5,000 and the synaptobrevin-to-lipid ratio to 1:10,000 led to almost no Ca^{2+}-independent fusion of VSyt1-liposomes with dT-liposomes, but Ca^{2+} addition led to efficient fusion (Fig. 3*E*, gray curve). Fusion of VSyt1-liposomes with T-liposomes still remained inefficient (Fig. 3*E*, orange curve; quantification in Fig. 3*F*).

All these assays reveal a much stronger activity of dT-liposomes than T-liposomes, showing that membrane anchoring of SNAP-25 dramatically enhances fusion efficiency. These enhancements do not arise from a better incorporation of dSNAP-25 on the dT-liposomes than SNAP-25 on the T-liposomes, as SDS-PAGE showed that the amount of reconstituted SNAP-25 tended to be equal or higher than that of reconstituted dSNAP-25 (*SI Appendix*, Figs. S2 and S3). Hence, this stimulation most likely arises from the fact that dSNAP-25 can remain bound to the dT-liposomes even after dissociation from syntaxin-1 during the preincubation with Munc18-1, NSF, and α-SNAP, whereas soluble SNAP-25 is released from the T-liposomes during the preincubation. Thus, the high local concentration of dSNAP-25 on the dT-liposomes dramatically facilitates binding of dSNAP-25 to synaptobrevin and syntaxin-1 on the template complex that they form with Munc18-1, leading to efficient SNARE complex assembly. It appears that, when there are sufficient synaptobrevin and syntaxin-1 molecules available, the number of SNARE complexes assembled in the absence of Ca^{2+} is sufficient to cause fusion. However, fusion requires Ca^{2+} when the numbers of synaptobrevin and syntaxin-1 molecules are very low and, correspondingly, the number of SNARE complexes that can be assembled is more limited.

Synergy between Syt1 and Membrane Anchoring of SNAP-25. Our results show that efficient Ca^{2+}-dependent fusion can be achieved in the presence of dSNAP-25, Munc18-1, Munc13-1C, NSF, α-SNAP, and Syt1 even at very low synaptobrevin-to-lipid and syntaxin-1–to–lipid ratios. To test whether Syt1 is important for fusion efficiency under these conditions, we performed fusion assays with dT-liposomes bearing a 1:5,000 syntaxin-1–to–lipid ratio and V- or VSyt1-liposomes containing a 1:10,000 synaptobrevin-to-lipid ratio, in the presence of Munc18-1, Munc13-1C, NSF, and α-SNAP. To estimate the relative amounts of proteins in the lumen and on the liposome surface existing at these P:L ratios, we performed proteolysis experiments with the dT-liposomes as well as with V- and VSyt1-liposomes analogous to those used for the fusion assays but containing a synaptobrevin L26C mutant that was labeled with Alexa 488, as synaptobrevin is difficult to visualize at these low densities. Analyses of the liposomes by SDS-PAGE followed by fluorescence imaging and Coomassie Blue staining (*SI Appendix*, Fig. S4 *A* and *B*) showed that about 80% of syntaxin-1 and dSNAP-25 are exposed on the surface of the dT-liposomes, while about 80% of synaptobrevin and more than 90% of Syt1 are exposed on the surface of the various V- and VSyt1-liposomes. Since our reconstitutions yield liposomes of about 100 nm diameter (32), which contain about 100,000 lipids, these results imply that the dT-liposomes with these P:L ratios contain about 16 syntaxin-1 molecules on their surface, and V- or VSyt1-liposomes contain about eight exposed synaptobrevin molecules.

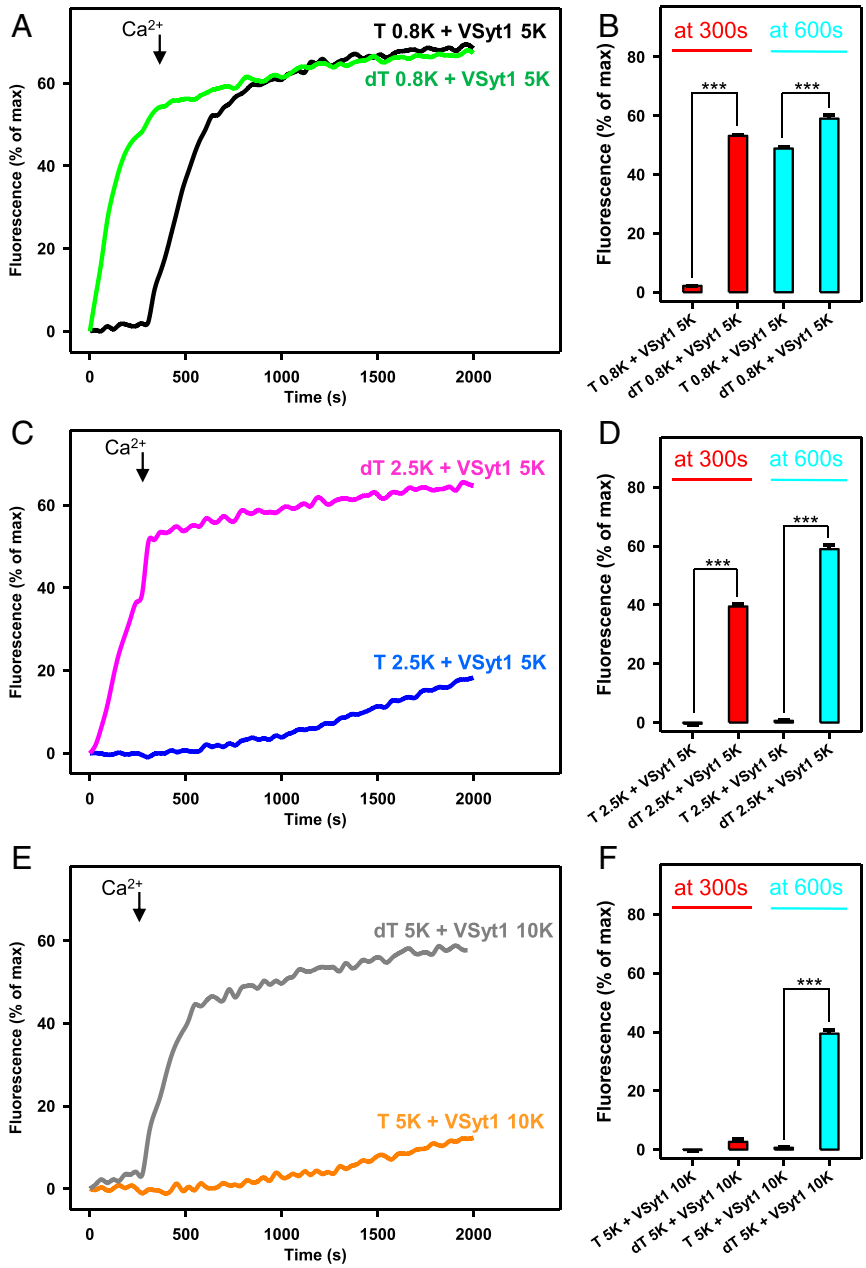

Fig. 3. Enhancement of liposome fusion by membrane anchoring of SNAP-25 at different synaptobrevin and syntaxin-1 densities. (*A*, *C*, and *E*) Content mixing between VSyt1-liposomes and T- or dT-liposomes was monitored from the increase in the fluorescence signal of Cy5-streptavidin trapped in the VSyt1-liposomes caused by FRET with PhycoE-biotin trapped in the T- or dT-liposomes upon liposome fusion. In the VSyt1-liposomes, the Syt1-to-lipid ratio was 1:1,000 and the synaptobrevin-to-lipid ratio was 1:5,000 (*A* and *C*) or 1:10,000 (*E*) (VSyt1 5K or VSyt1 10K, respectively). In the dT-liposomes, the dSNAP-25–to–lipid ratio was 1:800. In the T- and dT-liposomes, the syntaxin-1–to–lipid ratio was 1:800 (T 0.8K and dT 0.8K, respectively) (*A*), 1:2,500 (T 2.5K and dT 2.5K, respectively) (*C*), or 1:5,000 (T 5K and dT 5K, respectively) (*E*). The assays were performed in the presence of 1 μM Munc18-1, 0.2 μM Munc13-1C, 0.4 μM NSF, 2 μM α-SNAP, 5 μM excess SNAP-25 (only for experiments performed with T-liposomes), and 5 μM streptavidin. Experiments were started in the presence of 100 μM EGTA, and Ca^{2+} (600 μM) was added at 300 s. (*B*, *D*, and *F*) Quantification of the content mixing assays shown in *A*, *C*, and *E*. Bars represent averages of the normalized fluorescence intensities observed in the content mixing assays at 300 s (i.e., before Ca^{2+} addition) and at 600 s (i.e., 300 s after Ca^{2+} addition), performed in triplicates. Error bars represent SDs. Statistical significance and *P* values were determined by one-way ANOVA with the Holm–Sidak test (***$P < 0.001$).

At these protein densities, fusion of VSyt1-liposomes with dT-liposomes was much more efficient than that observed with the V-liposomes (Fig. 4*A*, black and green curves, respectively; Fig. 4*B*), showing again that Syt1 strongly stimulates fusion at very low SNARE densities. Control experiments where either Munc18-1, Munc13-1C, NSF, α-SNAP, or ATP were omitted individually showed that each one of these factors is required for the efficient Ca^{2+}-dependent fusion observed between VSyt1- and dT-liposomes (*SI Appendix*, Fig. S4 *C* and *D*). Additional experiments with VSyt1-liposomes bearing mutations in the Ca^{2+}-binding sites of the C_2A or C_2B domain confirmed that Ca^{2+} binding to both domains is important for the stimulation of fusion by Syt1 under these conditions (Fig. 4*A*, blue and pink curves; Fig. 4*B*), as observed in the experiments of Fig. 1 *C* and *D*. Interestingly, the low efficiencies of fusion observed in the absence of Syt1 (Fig. 4*A*, green curve) or with soluble SNAP-25

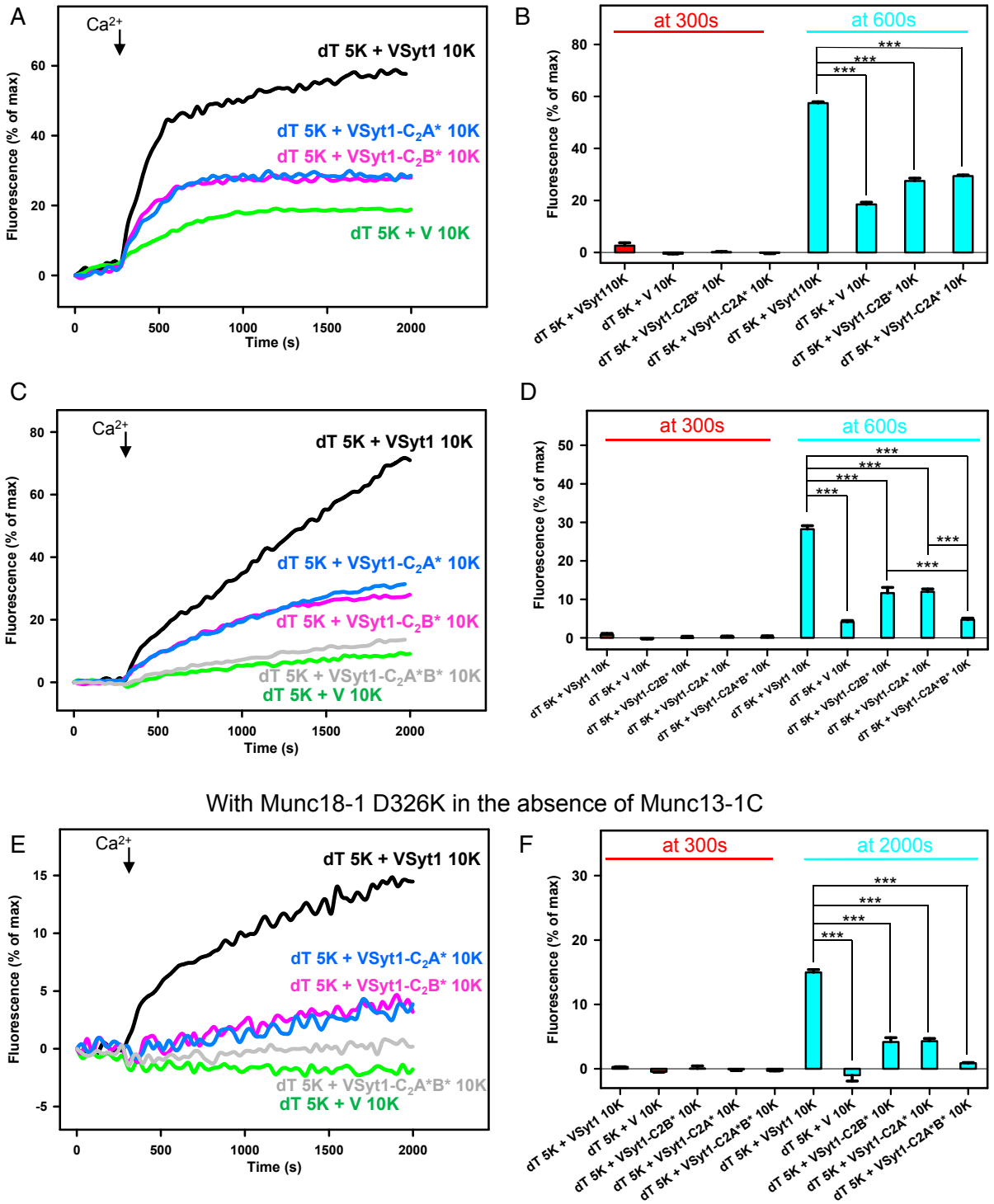

Fig. 4. Synergy between Syt1 and membrane anchoring of SNAP-25 in promoting liposome fusion at very low synaptobrevin and syntaxin-1 densities. (*A* and *C*) Content mixing between V- or VSyt1-liposomes and dT-liposomes (dT 5K) was monitored from the increase in the fluorescence signal of Cy5-streptavidin trapped in the V- or VSyt1-liposomes caused by FRET with PhycoE-biotin trapped in the dT-liposomes upon liposome fusion. The VSyt1 liposomes contained WT Syt1 or Syt1-bearing mutations in the Ca^{2+}-binding sites of the C_2A domain or the C_2B domain (VSyt1 10K, VSyt1-C_2A* 10K, or VSyt1-C_2B* 10K, respectively). The synaptobrevin-to-lipid ratio in V- and VSyt1-liposomes was 1:10,000, and the Syt1-to-lipid ratio in VSyt1-liposomes was 1:1,000. In dT-liposomes, the syntaxin-1–to–lipid ratio was 1:5,000 and the dSNAP-25–to–lipid ratio was 1:800. The assays were performed in the presence of 1 μM Munc18-1, 0.2 μM Munc13-1C, 0.4 μM NSF, 2 μM α-SNAP, and 5 μM streptavidin. The assays of *A* and *C* were performed under analogous conditions with different preparations. In *C*, experiments with VSyt1 liposomes bearing mutations in the Ca^{2+}-binding sites of both C_2 domains (VSyt1-C_2A*B* 10K) were also included. (*E*) Content mixing assays analogous to those shown in *A* and *C* but omitting Munc13-1C and replacing WT Munc18-1 with Munc18-1 D326K. All experiments were started in the presence of 100 μM EGTA, and Ca^{2+} (600 μM) was added at 300 s. (*B*, *D*, and *F*) Quantification of the content mixing assays shown in *A*, *C*, and *E*. Bars represent averages of the normalized fluorescence intensities observed in the content mixing assays at 300 s (i.e., before Ca^{2+} addition) and at 600 s (i.e., 300 s after Ca^{2+} addition), performed in triplicates. Error bars represent SDs. Statistical significance and *P* values were determined by one-way ANOVA with the Holm–Sidak test (***$P < 0.001$).

in the presence of Syt1 (Fig. 3*E*, orange curve) show that both Syt1 and membrane anchoring of SNAP-25 are critical for efficient fusion under these conditions and, therefore, that there is a strong synergy between the two proteins. We also note that it is common to observe some variability in results obtained with different liposome preparations in reconstitution assays of membrane fusion (47). Hence, it is important to perform repeat experiments with the same preparations for quantitative analyses (e.g., Fig. 4*B*) and to confirm that the relative extent of fusion observed under different conditions can be reproduced with different preparations. We find that this is particularly important when using very low P:L ratios, as there is larger variability in the activity of the liposomes. This variability is illustrated by the fusion assays shown in Fig. 4 *C* and *D*, which were performed with different liposome preparations containing the same P:L ratios as those of Fig. 4 *A* and *B* and exhibited less efficient fusion. However, the relative effects caused by removal of Syt1 or by mutations in the Ca^{2+}-binding sites of its C_2A or C_2B domain were comparable. In this set of experiments, we also included VSyt1-liposomes with mutations in the Ca^{2+}-binding sites of both C_2 domains (Fig. 4*C*, gray curve; Fig. 4*D*) and observed that these mutations again abolished stimulation of fusion by Syt1 completely.

While mammalian Munc13s and their invertebrate homolog unc-13 are normally essential for neurotransmitter release (30, 31), the total abrogation of neurotransmitter release observed in their absence can be partially rescued by distinct mutations designed to facilitate SNARE complex formation (2), including a gain-of-function mutation in Munc18-1 (22). Correspondingly, gain-of-function mutations in Munc18-1 partially overcome the requirement of Munc13-1C for fusion in our assays (16, 22). Hence, this reconstitution system provides an avenue to study how Munc13 function can be bypassed and to analyze fusion in the absence of any effects from Ca^{2+} binding to the Munc13-1C C_2B domain. To test whether liposome fusion can still be observed at very low synaptobrevin and syntaxin-1 densities in the absence of Munc13-1C, we performed fusion assays with dT-liposomes bearing a 1:5,000 syntaxin-1–to–lipid ratio and V- or VSyt1-liposomes containing a 1:10,000 synaptobrevin-to-lipid ratio in the presence of NSF, α-SNAP, and the gain-of-function Munc18-1 mutant D326K (16). We observed slow Ca^{2+}-dependent fusion between VSyt1-liposomes and dT-liposomes, but not between V-liposomes and dT-liposomes, and fusion involving the VSyt1-liposomes was disrupted by mutations in the Ca^{2+}-binding sites of both C_2 domains (Fig. 4 *E* and *F*). Hence, fusion can indeed be observed with such low synaptobrevin and syntaxin-1 densities in the absence of Munc13-1C, but Syt1 is required for fusion under these conditions, and fusion depends on Ca^{2+} binding to both Syt1 C_2 domains.

Discussion

Fusion assays with reconstituted proteoliposomes provide a powerful tool to investigate the mechanism of neurotransmitter release, but faithful recapitulation of the events that lead to Ca^{2+}-evoked synaptic vesicle fusion is challenging because of the complexity of this exquisitely regulated process. Studies showing that highly efficient Ca^{2+}-dependent liposome fusion could be observed with Munc18-1, Munc13-1C, NSF, α-SNAP, and the three neuronal SNAREs represented a milestone because they explained the essential nature of Munc18-1 and Munc13s for neurotransmitter release (9, 32). However, the high fusion efficiency observed in these assays prevented analysis of how the Ca^{2+} sensor Syt1 affects fusion. Here, we addressed this question and examined whether liposome fusion could be achieved with very low synaptobrevin and syntaxin-1 densities, which may allow to better reproduce the states that lead to neurotransmitter release in neurons. Importantly, we show that liposome fusion in the presence of Munc18-1, Munc13-1C, NSF, and α-SNAP is strongly stimulated by Syt1 at low synaptobrevin-to-lipid ratios and that such stimulation depends on Ca^{2+} binding to both Syt1 C_2 domains. We also show that anchoring SNAP-25 on the T-liposomes dramatically enhances fusion and exhibits a marked synergy with Syt1, allowing highly efficient Ca^{2+}-dependent fusion with a few SNARE complexes in a Syt1-, Munc18-1-, and Munc13-1C–dependent manner. These reconstitutions with the eight most central components of the neuronal exocytotic machinery provide a powerful framework to further investigate the mechanism of neurotransmitter release.

Presynaptic active zones constitute minimal computational units of the brain where synaptic vesicles fuse to release neurotransmitters, and the release probability is exquisitely controlled through a variety of presynaptic plasticity processes that underlie multiple forms of information processing in the brain (1, 48). Hence, synaptic vesicle fusion depends on a delicate balance between inhibitory and stimulatory interactions among the components of the release machinery, many of which perform both active and inhibitory roles (2). Munc18-1 hinders formation of the SNARE complex by binding to the closed conformation of syntaxin-1 (19) but constitutes a template to assemble the SNARE complex in downstream events (14–17). Munc13-1 helps to open syntaxin-1 to form the SNARE complex (19, 20) while bridging the vesicle and plasma membranes (18), but such bridging appears to occur in at least two orientations: 1) an approximately perpendicular orientation that is favored in the absence of Ca^{2+} and keeps the membranes apart, promoting SNARE complex assembly but to a limited extent; and 2) a more slanted orientation induced by Ca^{2+} binding to the Munc13-1C C_2B domain that promotes SNARE complex assembly more efficiently and facilitates membrane fusion (10, 33). This second, active orientation is also favored by binding of the C_1 domain to diacylglycerol and the C_2B domain to phosphatidylinositol 4,5-bisphosphate (PIP_2, and is likely stabilized during short-term plasticity processes that depend on Munc13-1 (34, 49). Hence, the number of SNARE complexes that are preassembled for each primed vesicle before Ca^{2+} influx is most likely controlled by energy barriers imposed by the same proteins that orchestrate SNARE complex assembly (Munc18-1 and Munc13-1) and perhaps by other factors, therefore preventing uncontrolled fusion that would result if too many SNARE complexes were formed. The much more efficient SNARE complex assembly that can occur in the presence of Ca^{2+} is limited because the intracellular Ca^{2+} concentration is elevated only for a very short time after Ca^{2+} influx but is facilitated when Ca^{2+} accumulates during repetitive stimulation, increasing the priming and fusion efficiency.

In our previous studies of liposome fusion in the presence of Munc18-1, Munc13-1C, NSF, and α-SNAP, but not Syt1, the V- and T-liposomes were typically prepared with 1:500 and 1:800 P:L ratios, respectively, and therefore contained about 200 copies of synaptobrevin and 125 copies of syntaxin-1 (assuming a 100-nm diameter). Under these conditions, a few SNARE complexes are assembled in the absence of Ca^{2+}, and SNARE complex assembly is dramatically enhanced by addition of Ca^{2+} (10, 32), resulting in highly efficient Ca^{2+}-dependent fusion. The stimulation of fusion by Ca^{2+} in these assays likely reflects events that occur during synaptic vesicle priming and fusion and that are facilitated during repetitive stimulation but cannot be resolved in the time scale of our measurements. Because of the high fusion efficiency, it was impossible to observe stimulatory effects on Ca^{2+}-dependent fusion by Syt1 or any other factor under these conditions. These arguments led us to test whether a stimulatory effect of Syt1 in our fusion assays could be uncovered by lowering the SNARE densities on the liposomes and therefore limiting the number of SNARE complexes that could be formed at any given time. Indeed, we observed a strong stimulation of Ca^{2+}-dependent liposome fusion by Syt1 when we lowered the synaptobrevin-to-protein ratio to 1:10,000 (Fig. 1). Such stimulation

was Ca^{2+} dependent and was disrupted by mutations in the Ca^{2+}-binding sites of the Syt1 C_2 domains (Fig. 1). Note also that the fusion observed in these assays requires both Munc18-1 and Munc13C (Fig. 1) and that only about eight synaptobrevin molecules are available on the surface of the liposomes (see above). These observations show that in these assays, fusion is mediated by a few SNARE complexes that are assembled via a Munc18-1–Munc13-1C–dependent pathway and is stimulated by Ca^{2+} binding to the Syt1 C_2 domains. Hence, these reconstitution assays recapitulate several fundamental features of neurotransmitter release in neurons. It is still unclear how Syt1 stimulates fusion, but recent data suggested a mechanism whereby Syt1 is bound to the SNARE complex before Ca^{2+} influx and Ca^{2+} releases the Syt1-SNARE interaction, inducing a specific Ca^{2+}- and PIP_2-dependent interaction with the plasma membrane and allowing cooperation between the SNAREs and Syt1 in fast membrane fusion (26).

Our results also show that membrane anchoring of SNAP-25 dramatically enhances liposome fusion (Figs. 2 and 3). Previous studies had shown that such anchoring enhanced fusion mediated by the SNAREs alone because it facilitated formation of a syntaxin-1–SNAP-25 acceptor complex (46). However, fusion stimulation by membrane anchoring of SNAP-25 could not occur by this mechanism in our assays because they were performed in the presence of NSF and α-SNAP, which disassemble syntaxin-1-SNAP-25 complexes (9). Rather, fusion stimulation can be attributed to the drastic increase in the local concentration of SNAP-25 upon anchoring to the syntaxin-1–containing liposomes, which is expected to greatly facilitate binding of SNAP-25 to synaptobrevin and syntaxin-1 when they form the template complex with Munc18-1 (14–17). It is worth noting that SNAP-25 was reported to form a tripartite complex with syntaxin-1 and Munc18-1 (50), but the nature of this tripartite complex is highly unclear, as the interactions between the syntaxin-1 and SNAP-25 SNARE motifs observed in the SNARE complex (7) are incompatible with those present in the closed syntaxin-1–Munc18-1 complex (13). Moreover, incubation of liposomes containing syntaxin-1–SNAP-25 heterodimers with NSF, α-SNAP, and Munc18-1 releases SNAP-25 from the liposomes, leading to formation of the binary syntaxin-1–Munc18-1 complex (9). Our results also argue against formation of the SNAP-25–syntaxin-1–Munc18-1 tripartite complex, as such a complex would already localize SNAP-25 to the membrane, and thus, membrane anchoring of SNAP-25 would not be expected to increase fusion so dramatically.

Membrane anchoring of SNAP-25 allowed highly efficient Ca^{2+}-independent fusion at moderate synaptobrevin and syntaxin-1 P:L ratios (1:1,000 and 1:800, respectively) even without Syt1 (Fig. 2), but fusion became more Ca^{2+} dependent at lower synaptobrevin and syntaxin-1 densities (Fig. 3). Efficient Ca^{2+}-dependent fusion at synaptobrevin-to-lipid ratio 1:10,000 and syntaxin-1–to–lipid ratio 1:5,000 required both Syt1 and membrane anchoring of SNAP-25 (Fig. 4*A*). These results reveal an intriguing synergy between Syt1 and membrane anchoring of SNAP-25. It is plausible that this synergy arises in part because Syt1 also facilitates trans-SNARE complex assembly in the absence of Ca^{2+} (10), which may underlie the role of Syt1 in synaptic vesicle priming (51, 52). However, fusion stimulation by Syt1 depends on Ca^{2+} binding to its C_2 domains, which is not expected to facilitate assembly. Hence, it seems likely that the synergy arises also from cooperativity between two separate effects, that is, the enhancement of SNARE complex assembly by membrane anchoring of SNAP-25 and the stimulatory effect of Syt1 on fusion itself. As explained above, there is a balance between inhibitory and stimulatory interactions, and the efficiency of fusion depends on this balance. In the absence of Ca^{2+}, Munc18-1 and Munc13-1C promote SNARE complex assembly, but at the same time Munc13-1C likely hinders fusion, and SNARE complex assembly is less efficient than in the presence of Ca^{2+}. As a result, fusion is Ca^{2+} dependent when the number of SNARE complexes assembled before Ca^{2+} addition is insufficient, but efficient Ca^{2+}-independent fusion occurs when SNARE complex assembly is enhanced by gain-of-function mutants of Munc18-1 (16, 22) or by membrane anchoring of SNAP-25. The stimulatory activity of Syt1 is not required for fusion when there are enough SNARE complexes assembled but becomes critical with fewer SNARE complexes.

While our reconstitution results are satisfying because they correlate with multiple features of neurotransmitter release in vivo, further studies will be required to understand other aspects of release. Thus, while the similar impairments in fusion caused by mutations in the Ca^{2+}-binding sites of both Syt1 C_2 domains (Figs. 1 and 4) agree with the fact that both C_2 domains are important for release, mutations in the C_2B domain Ca^{2+}-binding sites disrupt release more strongly in vivo (44, 53). It is plausible that this discrepancy arises because the strong disruption of release caused by mutations in the Syt1 C_2B domain Ca^{2+}-binding sites may be due, in part, to a dominant negative effect that requires complexins (53), proteins that enhance Ca^{2+}-triggered neurotransmitter release (54) and were not included in our assays. In preliminary experiments, we have not been able to observe stimulatory effects of complexin-1, and it has been generally difficult to observe such stimulatory effects in bulk fusion assays reported in the literature. Stimulation of fusion by complexin-1 was observed in single-vesicle fusion assays that did not include Munc18-1, NSF, α-SNAP, and Munc13-1C (55–57), or included Munc18-1, NSF, α-SNAP, and a Munc13-1 fragment that lacks the C_2C domain (58) and is much less active than Munc13-1C (32). Since complexin-1 prevents the disassembly of trans-SNARE complexes by NSF-α-SNAP (10), it is plausible that this activity underlies the decrease of neurotransmitter release observed in the absence of complexins (54), and the observation of a stimulatory role in our assays may require a careful adjustment of the concentrations of Munc18-1, NSF, α-SNAP, and Munc13-1C to have the proper balance between trans-SNARE complex disassembly and reassembly. Elucidating the effects of multiple lipids on exocytosis will also require further study. For instance, sphingolipids are abundant brain lipids that were not included in our reconstitutions, and the cholesterol concentrations in synaptic vesicles and the presynaptic plasma membrane (37, 38) are higher than those present in our liposomes. These lipids can cluster in membrane domains where SNAREs accumulate (59), which may increase their activity or potentially sequester them. Note also that the time scale of our assays (seconds) does not allow resolution of the fusion step from upstream events, such as tethering and priming. Nevertheless, these bulk fusion assays have provided a wealth of information on the mechanism of neurotransmitter release that can be used to improve other assays that have faster time resolution, as was done recently with single-vesicle fusion experiments (58). Thus, the results described here provide a framework to make further advances in this field through reconstitution and many other approaches.

Methods

Protein Expression and Purification. The proteins used in this study included the following: full-length rat syntaxin-1, full-length rat SNAP-25A (WT and C84S,C85S,C90S,C92S mutant), full-length rat synaptobrevin-2, full-length rat Munc18-1 (WT and D326K mutant), rat synaptotagmin-1 57 to 421 (cysteine-free mutant without and with D178A,D230A,D232A, D309A,D363A,D365A, or D178A,D230A,D232A,D309A,D363A,D365A mutations), full-length *Cricetulus griseus* NSF, full-length Bos Taurus α-SNAP, and a rat Munc13-1 fragment spanning the C_1, C_2B, MUN, and C_2C domains (Munc13-1C; residues 529 to 1725, Δ1408 to 1452). Expression vectors for these proteins, as well as methods to express them in *Escherichia coli* BL21 (DE3) cells and purify them, were described previously (9, 10, 12, 16, 18, 32). Briefly, syntaxin-1 was purified using HisPur Ni-NTA Resin (Thermo Fisher) in 20 mM Tris, pH 7.4, 500 mM NaCl,

8 mM imidazole, 2% Triton X-100 (vol/vol), and 6 M urea, followed by elution in 20 mM Tris, pH 7.4, 500 mM NaCl, 400 mM imidazole, and 0.1% dodecylphosphocholine (DPC). The polyhistidine tag was removed using thrombin, followed by size-exclusion chromatography on a Superdex 200 column (GE 10/300) equilibrated in 20 mM Tris, pH 7.4, 125 mM NaCl, 1 mM Tris(2-carboxyethyl)phosphine (TCEP), and 0.2% DPC. The cysteine-free variant of SNAP-25 was purified using HisPur Ni-NTA Resin (Thermo Fisher) in 50 mM Tris, pH 8.0, 500 mM NaCl, 20 mM imidazole, and 1% Triton X-100 (vol/vol). The His_6-tag was cleaved by thrombin, and the protein was further purified by size-exclusion chromatography using a Superdex 75 column (GE 16/60) in 50 mM Tris, pH 8.0, and 150 mM NaCl. For WT SNAP-25, the elution buffer contained 0.1% DPC instead of 1% Triton X-100 (vol/vol). Dodecylation of WT SNAP-25 was performed as described (46). Purification of full-length synaptobrevin-2 was carried out using Glutathione Sepharose 4B resin (GE) at 4 C. The bound proteins were washed with phosphate-buffered saline (PBS) with 1% Triton X-100 (vol/vol) followed by the addition of thrombin to remove the glutathione-S-transferase (GST)-tag. Final purification involved cation exchange chromatography on a HiTrap SP column (GE) in 25 mM NaAc, pH 5.5, 1 mM TCEP, and 1% β-octyl glucoside (β-OG) (wt/vol) using a linear gradient from 0 to 1 M NaCl. Full-length Munc18-1 was purified on Glutathione Sepharose 4B resin (GE) at 4 C, and the bound proteins were treated with PBS, PBS with 1% Triton X-100 (vol/vol), and PBS with 1 M NaCl. The GST-tag was cleaved with thrombin followed by immediate size-exclusion chromatography on a Superdex 200 column (GE 16/60) in a buffer containing 20 mM Tris, pH 7.4, 200 mM KCl, and 1 mM TCEP. The Munc18-1 D326K mutant was purified by the same procedures. His_6-synaptotagmin-1 57 to 421 was obtained from the soluble fraction of the cell lysate that was subsequently mixed with 1.5% Triton X-100 (vol/vol) and stirred at 4 C for 2 h. Upon further centrifugation, the supernatant was incubated with PurHis Ni-NTA resin (Thermo Fisher) at 4 C for 2 h. The resin was washed with 25 mM Hepes, pH 7.4, 600 mM KCl, 10 mM imidazole, and 1% β-OG (wt/vol). Final purification was performed using size-exclusion chromatography on a Superdex 200 column (GE 16/60) in 25 mM Hepes, pH 7.4, 600 mM KCl, and 1% β-OG (wt/vol). The proteins bearing mutations in the C_2A and/or C_2B domain Ca^{2+}-binding sites (D178A,D230A,D232A, D309A,D363A,D365A, or D178A,D230A,D232A,D309A,D363A,D365A) were purified following the same protocol. Full-length NSF was obtained by affinity purification on HisPur Ni-NTA resin (Thermo Fisher) followed by size-exclusion chromatography of hexameric NSF on a Superdex S200 column (GE 16/60) in 50 mM Tris, pH 8.0, 100 mM NaCl, 1 mM ATP, 1 mM ethylenediaminetetraacetic acid (EDTA), 1 mM dithiothreitol, and 10% glycerol (vol/vol). Upon *Tobacco Etch Virus* (TEV) protease and apyrase treatment, the hexameric form of NSF was separated from the monomer by three rounds of size-exclusion chromatography on a Superdex S200 column (GE 16/60) in 50 mM NaPi, pH 8.0, 100 mM NaCl, and 0.5 mM TCEP. Final reassembly with the monomers and gel filtration chromatography of reassembled hexameric NSF were performed using a Superdex S200 column (GE 16/60) in 50 mM Tris, pH 8.0, 100 mM NaCl, 1 mM ATP, 1 mM EDTA, 1 mM TCEP, and 10% glycerol (vol/vol). Munc13-1C (residues 529 to 1725, Δ1408 to 1452) was purified using HisPur Ni-NTA resin (Thermo Fisher) and washed with 50 mM Tris, pH 8, 10 mM imidazole, 750 mM NaCl, 1 mM TCEP, and 10% glycerol (vol/vol). Upon elution, the protein was dialyzed overnight at 4 C in 50 mM Tris, pH 8, 250 mM NaCl, 1 mM TCEP, 2.5 mM CaCl2, and 10% glycerol (vol/vol) in the presence of thrombin. The protein was further purified by anion exchange chromatography on a HiTrap Q column (GE) in 20 mM Tris, pH 8.0, 1 mM TCEP, and 10% glycerol (vol/vol) using a linear gradient from 0 to 1 M NaCl.

Content Mixing Assays. The assays were performed basically as reported (47) with a few modifications as described below. V-liposomes containing full-length synaptobrevin-2 (P:L ratio 1:1,000, 1:5,000, or 1:10,000) were made with 39% POPC (1-palmitoyl, 2-oleoyl phosphatidylcholine), 19% DOPS (1,2-dioleoyl-sn-glycero-3-phospho-L-serine), 19% POPE (1-palmitoyl-2-oleoyl-sn-phosphatidylethanolamine), 20% cholesterol, 1.5% NBD-PE (*N*-(7-nitrobenz-2-oxa-1,3-diazol-4-yl)-1,2-dihexadecanoyl-sn-glycero-3-phosphoethanolamine, triethylammonium salt), and 1.5% Marina Blue DHPE (1,2-dihexadecanoyl-sn-glycero-3-phosphoethanolamine). VSyt1-liposomes containing synaptotagmin-1 57 to 421 (P:L ratio 1:1,000) and full-length synaptobrevin (P:L ratio 1:1,000, 1:5,000, or 1:10,000) contained 40% POPC, 6.8% DOPS, 30.2% POPE, 20% cholesterol, 1.5% NBD-PE, and 1.5% Marina Blue DHPE. T-liposomes containing syntaxin-1 and cysteine-free SNAP-25 (syntaxin-1:lipid ratio 1:800, 1:2,500, or 1:5,000) and dT-liposomes containing dSNAP-25 (P:L ratio 1:800) and syntaxin-1 (P:L ratio 1:800, 1:2,500, or 1:5,000) were made with 38% POPC, 18% DOPS, 20% POPE, 20% cholesterol, 2% PIP2 (phosphatidylinositol 4,5-biphosphate), and 2% DAG (diacylglycerol). For T-liposomes, SNAP-25 was included during reconstitution at a concentration that was fivefold the syntaxin-1 concentration. Dried lipid films were resuspended in 25 mM Hepes, pH 7.4, 150 mM KCl, 1 mM TCEP, 10% glycerol (vol/vol), and 2% β-OG. Lipid solutions were then mixed with the respective proteins and with 4 μM phycoerythrin-biotin for T- or dT-liposomes or with 8 μM Cy5-streptavidin for V- or VSyt1-liposomes in 25 mM Hepes, pH 7.4, 150 mM KCl, 1 mM TCEP, and 10% glycerol (vol/vol). Proteoliposomes were prepared by detergent removal using dialysis with 2 g/L Amberlite XAD-2 beads (Sigma) three times at 4 C and subsequent cofloatation on a three-layer Histodenz gradient (35%, 25%, and 0%) and harvested from the topmost layer. Although liposomes prepared by these procedures allow simultaneous monitoring of lipid mixing from dequenching of Marina Blue fluorescence and content mixing from the increase in Cy5 fluorescence due to development of FRET with phycoerythrin, lingering intermittent problems with our spectrofluorometer prevented us from consistently obtaining lipid mixing data of sufficient quality. Hence, in this study, we focused on measuring content mixing (excitation at 565 nm, emission at 670 nm), which provides the more reliable means to monitor liposome fusion. Each reaction was prepared in a total volume of 200 μl with V- or VSyt1-liposomes (0.125 mM total lipid), T or dT-liposomes (0.25 mM total lipid), 2.5 mM $MgCl_2$, 2 mM ATP, 0.1 mM EGTA, 5 μM streptavidin, 5 μM SNAP-25 (only for reactions with T-liposomes), 0.4 μM NSF, 2 μM α-SNAP, 1 μM Munc18-1, and 0.2 μM Munc13-1C in different combinations as described in the figure legends. At 300 s, 0.6 mM $CaCl_2$ was added to each reaction. Experiments were repeated at least three times with a given preparation, and the results were verified in multiple experiments performed with different preparations. All assays were performed at 30 C using a PTI QuantaMaster 400 spectrofluorometer (T-format) equipped with a rapid Peltier temperature-controlled four-position sample holder. Content mixing signals were normalized to the maximum signals obtained by the addition of 1% β-OG to control reactions acquired without streptavidin to measure the maximal Cy5 fluorescence.

Limited Proteolysis of Liposomes. Proti-Ace Kit by Hampton Research was used to perform proteolysis of the following liposomes: V-liposomes containing full-length synaptobrevin-2 L26C prelabeled with Alexa 488 as described (10) (P:L ratio 1:10,000); VSyt1-liposomes containing Alexa488-labeled synaptobrevin L26C (P:L ratio 1:10,000) and synaptotagmin-1 57 to 421 WT or D178A,D230A,D232A, D309A,D363A,D365A, or D178A,D230A,-D232A,D309A,D363A,D365A mutants (P:L ratio 1:1,000); and dT-liposomes containing syntaxin-1 (P:L ratio 1:5,000) and dSNAP-25 (P:L ratio 1:800). For this purpose, 20 μl liposomes (2.5 mM lipid) were mixed either with 60 μl buffer (25 mM Hepes, pH 7.4, 150 mM KCl, and 1 mM TCEP) or with 60 μl six Proti-Ace enzymes (10 μl of 0.01 mg/mL stock of each protease reagent) and incubated at 37 C for 5 h. The reaction was stopped by addition of SDS-PAGE sample buffer, and the digests were separated by SDS-PAGE. The gel was analyzed with a ChemiDoc imager using emission and excitation filters to detect Alexa 488 and later was stained with Coomassie Blue. The amounts of proteins were estimated from the gel images with ImageLab.

Data Availability. All the data presented in this study are included in the article text, *SI Appendix*, and Dataset_S1.

ACKNOWLEDGMENTS. We thank Junjie Xu for fruitful discussions. This work was supported by Grant I-1304 from the Welch Foundation (to J.R.) and by NIH Research Project Award R35 NS097333 (to J.R.).

1. T. C. Südhof, Neurotransmitter release: The last millisecond in the life of a synaptic vesicle. *Neuron* **80**, 675–690 (2013).
2. J. Rizo, Mechanism of neurotransmitter release coming into focus. *Protein Sci.* **27**, 1364–1391 (2018).
3. A. T. Brunger, U. B. Choi, Y. Lai, J. Leitz, Q. Zhou, Molecular mechanisms of fast neurotransmitter release. *Annu. Rev. Biophys.* **47**, 469–497 (2018).
4. T. Söllner, M. K. Bennett, S. W. Whiteheart, R. H. Scheller, J. E. Rothman, A protein assembly-disassembly pathway in vitro that may correspond to sequential steps of synaptic vesicle docking, activation, and fusion. *Cell* **75**, 409–418 (1993).
5. P. I. Hanson, R. Roth, H. Morisaki, R. Jahn, J. E. Heuser, Structure and conformational changes in NSF and its membrane receptor complexes visualized by quick-freeze/deep-etch electron microscopy. *Cell* **90**, 523–535 (1997).
6. M. A. Poirier *et al.*, The synaptic SNARE complex is a parallel four-stranded helical bundle. *Nat. Struct. Biol.* **5**, 765–769 (1998).
7. R. B. Sutton, D. Fasshauer, R. Jahn, A. T. Brunger, Crystal structure of a SNARE complex involved in synaptic exocytosis at 2.4 A resolution. *Nature* **395**, 347–353 (1998).
8. A. Mayer, W. Wickner, A. Haas, Sec18p (NSF)-driven release of Sec17p (alpha-SNAP) can precede docking and fusion of yeast vacuoles. *Cell* **85**, 83–94 (1996).

9. C. Ma, L. Su, A. B. Seven, Y. Xu, J. Rizo, Reconstitution of the vital functions of Munc18 and Munc13 in neurotransmitter release. *Science* **339**, 421–425 (2013).
10. E. A. Prinslow, K. P. Stepien, Y. Z. Pan, J. Xu, J. Rizo, Multiple factors maintain assembled trans-SNARE complexes in the presence of NSF and αSNAP. *eLife* **8**, e38880 (2019).
11. U. B. Choi *et al*., NSF-mediated disassembly of on- and off-pathway SNARE complexes and inhibition by complexin. *eLife* **7**, e36497 (2018).
12. I. Dulubova *et al*., A conformational switch in syntaxin during exocytosis: Role of munc18. *EMBO J.* **18**, 4372–4382 (1999).
13. K. M. Misura, R. H. Scheller, W. I. Weis, Three-dimensional structure of the neuronal-Sec1-syntaxin 1a complex. *Nature* **404**, 355–362 (2000).
14. D. Parisotto *et al*., An extended helical conformation in domain 3a of Munc18-1 provides a template for SNARE (soluble N-ethylmaleimide-sensitive factor attachment protein receptor) complex assembly. *J. Biol. Chem.* **289**, 9639–9650 (2014).
15. R. W. Baker *et al*., A direct role for the Sec1/Munc18-family protein Vps33 as a template for SNARE assembly. *Science* **349**, 1111–1114 (2015).
16. E. Sitarska *et al*., Autoinhibition of Munc18-1 modulates synaptobrevin binding and helps to enable Munc13-dependent regulation of membrane fusion. *eLife* **6**, e24278 (2017).
17. J. Jiao *et al*., Munc18-1 catalyzes neuronal SNARE assembly by templating SNARE association. *eLife* **7**, e41771 (2018).
18. B. Quade *et al*., Membrane bridging by Munc13-1 is crucial for neurotransmitter release. *eLife* **8**, e42806 (2019).
19. C. Ma, W. Li, Y. Xu, J. Rizo, Munc13 mediates the transition from the closed syntaxin-Munc18 complex to the SNARE complex. *Nat. Struct. Mol. Biol.* **18**, 542–549 (2011).
20. X. Yang *et al*., Syntaxin opening by the MUN domain underlies the function of Munc13 in synaptic-vesicle priming. *Nat. Struct. Mol. Biol.* **22**, 547–554 (2015).
21. K. P. Stepien, E. A. Prinslow, J. Rizo, Munc18-1 is crucial to overcome the inhibition of synaptic vesicle fusion by αSNAP. *Nat. Commun.* **10**, 4326 (2019).
22. S. Park *et al*., UNC-18 and tomosyn antagonistically control synaptic vesicle priming downstream of UNC-13 in *Caenorhabditis elegans*. *J. Neurosci.* **37**, 8797–8815 (2017).
23. R. Fernández-Chacón *et al*., Synaptotagmin I functions as a calcium regulator of release probability. *Nature* **410**, 41–49 (2001).
24. J. S. Rhee *et al*., Augmenting neurotransmitter release by enhancing the apparent Ca2+ affinity of synaptotagmin 1. *Proc. Natl. Acad. Sci. U.S.A.* **102**, 18664–18669 (2005).
25. Q. Zhou *et al*., Architecture of the synaptotagmin-SNARE machinery for neuronal exocytosis. *Nature* **525**, 62–67 (2015).
26. R. Voleti, K. Jaczynska, J. Rizo, Ca^{2+}-dependent release of synaptotagmin-1 from the SNARE complex on phosphatidylinositol 4,5-bisphosphate-containing membranes. *eLife* **9**, e57154 (2020).
27. T. Weber *et al*., SNAREpins: Minimal machinery for membrane fusion. *Cell* **92**, 759–772 (1998).
28. W. C. Tucker, T. Weber, E. R. Chapman, Reconstitution of Ca2+-regulated membrane fusion by synaptotagmin and SNAREs. *Science* **304**, 435–438 (2004).
29. M. Verhage *et al*., Synaptic assembly of the brain in the absence of neurotransmitter secretion. *Science* **287**, 864–869 (2000).
30. J. E. Richmond, W. S. Davis, E. M. Jorgensen, UNC-13 is required for synaptic vesicle fusion in C. elegans. *Nat. Neurosci.* **2**, 959–964 (1999).
31. F. Varoqueaux *et al*., Total arrest of spontaneous and evoked synaptic transmission but normal synaptogenesis in the absence of Munc13-mediated vesicle priming. *Proc. Natl. Acad. Sci. U.S.A.* **99**, 9037–9042 (2002).
32. X. Liu *et al*., Functional synergy between the Munc13 C-terminal C1 and C2 domains. *eLife* **5**, e13696 (2016).
33. J. Xu *et al*., Mechanistic insights into neurotransmitter release and presynaptic plasticity from the crystal structure of Munc13-1 C_1C_2BMUN. *eLife* **6**, e22567 (2017).
34. O. H. Shin *et al*., Munc13 C2B domain is an activity-dependent Ca2+ regulator of synaptic exocytosis. *Nat. Struct. Mol. Biol.* **17**, 280–288 (2010).
35. M. Geppert *et al*., Synaptotagmin I: A major Ca2+ sensor for transmitter release at a central synapse. *Cell* **79**, 717–727 (1994).
36. M. Zick, W. Wickner, Improved reconstitution of yeast vacuole fusion with physiological SNARE concentrations reveals an asymmetric Rab(GTP) requirement. *Mol. Biol. Cell* **27**, 2590–2597 (2016).
37. S. Takamori *et al*., Molecular anatomy of a trafficking organelle. *Cell* **127**, 831–846 (2006).
38. B. G. Wilhelm *et al*., Composition of isolated synaptic boutons reveals the amounts of vesicle trafficking proteins. *Science* **344**, 1023–1028 (2014).
39. R. Mohrmann, H. de Wit, M. Verhage, E. Neher, J. B. Sørensen, Fast vesicle fusion in living cells requires at least three SNARE complexes. *Science* **330**, 502–505 (2010).
40. P. C. Zucchi, M. Zick, Membrane fusion catalyzed by a Rab, SNAREs, and SNARE chaperones is accompanied by enhanced permeability to small molecules and by lysis. *Mol. Biol. Cell* **22**, 4635–4646 (2011).
41. M. Zick, W. T. Wickner, A distinct tethering step is vital for vacuole membrane fusion. *eLife* **3**, e03251 (2014).
42. J. Ubach, X. Zhang, X. Shao, T. C. Südhof, J. Rizo, Ca2+ binding to synaptotagmin: How many Ca2+ ions bind to the tip of a C2-domain? *EMBO J.* **17**, 3921–3930 (1998).
43. I. Fernandez *et al*., Three-dimensional structure of the synaptotagmin 1 C2B-domain: Synaptotagmin 1 as a phospholipid binding machine. *Neuron* **32**, 1057–1069 (2001).
44. O. H. Shin, J. Xu, J. Rizo, T. C. Südhof, Differential but convergent functions of Ca2+ binding to synaptotagmin-1 C2 domains mediate neurotransmitter release. *Proc. Natl. Acad. Sci. U.S.A.* **106**, 16469–16474 (2009).
45. M. Veit, T. H. Söllner, J. E. Rothman, Multiple palmitoylation of synaptotagmin and the t-SNARE SNAP-25. *FEBS Lett.* **385**, 119–123 (1996).
46. A. J. Kreutzberger, B. Liang, V. Kiessling, L. K. Tamm, Assembly and comparison of plasma membrane SNARE acceptor complexes. *Biophys. J.* **110**, 2147–2150 (2016).
47. X. Liu *et al*., Simultaneous lipid and content mixing assays for in vitro reconstitution studies of synaptic vesicle fusion. *Nat. Protoc.* **12**, 2014–2028 (2017).
48. W. G. Regehr, Short-term presynaptic plasticity. *Cold Spring Harb. Perspect. Biol.* **4**, a005702 (2012).
49. J. S. Rhee *et al*., Beta phorbol ester- and diacylglycerol-induced augmentation of transmitter release is mediated by Munc13s and not by PKCs. *Cell* **108**, 121–133 (2002).
50. S. Jakhanwal, C. T. Lee, H. Urlaub, R. Jahn, An activated Q-SNARE/SM protein complex as a possible intermediate in SNARE assembly. *EMBO J.* **36**, 1788–1802 (2017).
51. T. Bacaj *et al*., Synaptotagmin-1 and -7 are redundantly essential for maintaining the capacity of the readily-releasable pool of synaptic vesicles. *PLoS Biol.* **13**, e1002267 (2015).
52. S. Chang, T. Trimbuch, C. Rosenmund, Synaptotagmin-1 drives synchronous Ca^{2+}-triggered fusion by C_2B-domain-mediated synaptic-vesicle-membrane attachment. *Nat. Neurosci.* **21**, 33–40 (2018).
53. Q. Zhou *et al*., The primed SNARE-complexin-synaptotagmin complex for neuronal exocytosis. *Nature* **548**, 420–425 (2017).
54. K. Reim *et al*., Complexins regulate a late step in Ca2+-dependent neurotransmitter release. *Cell* **104**, 71–81 (2001).
55. T. Y. Yoon *et al*., Complexin and Ca2+ stimulate SNARE-mediated membrane fusion. *Nat. Struct. Mol. Biol.* **15**, 707–713 (2008).
56. J. Diao *et al*., Synaptic proteins promote calcium-triggered fast transition from point contact to full fusion. *eLife* **1**, e00109 (2012).
57. J. Kim, Y. Zhu, Y. K. Shin, Preincubation of t-SNAREs with complexin I increases content-mixing efficiency. *Biochemistry* **55**, 3667–3673 (2016).
58. Y. Lai *et al*., Molecular mechanisms of synaptic vesicle priming by Munc13 and Munc18. *Neuron* **95**, 591–607.e10 (2017).
59. T. Lang *et al*., SNAREs are concentrated in cholesterol-dependent clusters that define docking and fusion sites for exocytosis. *EMBO J.* **20**, 2202–2213 (2001).